VUV radiation of high temperature CO 2 /Ar plasmas

Sean Mcguire, Augustin Tibère-Inglesse, Pierre Mariotto, Christophe O Laux, Brett A Cruden

VUV radiation of high temperature CO 2 /Ar plasmas

Sean Mcguire, Augustin Tibère-Inglesse, Pierre Mariotto, Christophe Laux, Brett Cruden

AIAA SciTech Forum
6-10 January 2020, Orlando, FL
AIAA Scitech 2020 Forum

10.2514/6.2020-0732

VUV radiation of high temperature CO_2/Ar plasmas

Sean D. McGuire*, Augustin Tibère-Inglesse†, Pierre Mariotto‡ and Christophe O. Laux§
Laboratoire EM2C, CNRS UPR288, CentraleSupélec, Université Paris Saclay
3 rue Joliot-Curie, Gif-sur-Yvette, France

Brett A. Cruden¶
AMA Inc. at NASA Ames Research Center
Moffett Field, CA 94035, USA

Optical emission measurements of CO 4th positive radiation, calibrated in absolute intensity, are compared with SPECAIR calculations done using the electronic transition moment function (ETMF) of Spielfiedel and Kirby and Cooper. The emission measurements are spectrally resolved and span the VUV and UV spectral regions, with a minimum reported wavelength of approximately 140 nm. The source for the CO 4th positive emission is an atmospheric plasma produced using an inductively coupled plasma torch facility. A mixture of CO_2 and Ar is injected and heated via the induction fields to produce the hot CO responsible for the observed 4th positive emission. The comparison between experimental measurements and SPECAIR calculations shows that the ETMF used reproduces well the observed emission.

I. Introduction

Radiative heat flux is expected to be an important contributor for manned space missions beyond Earth orbit, due to the large capsule size and high entry velocity associated with such missions.[1–4] In particular, radiative heat flux in the ultraviolet is expected to become significant for Mars and Venus entries at speeds above 7.5 km/s. The Pioneer Venus missions entered at velocities in excess of 11 km/s. Beyond direct entry scenarios, there is significant interest in using aerocapture maneuvers for missions to Mars and Venus in order to increase the percentage of useful payload.[3,5–7] Depending upon the specific parameters of this maneuver, the radiative heat flux can represent an important portion of the total heat flux. This will become even more important for the larger capsule sizes used for manned missions. For Venus and Mars atmospheres, composed primarily of CO_2, the CO($A\,^1\Pi \rightarrow X\,^1\Sigma^+$) transition, called the CO fourth positive system and noted CO(4+), represents either a significant or dominant portion of the radiative heat flux.[2,8] It is therefore important to validate the radiation models used for this system and to reduce the corresponding uncertainty.

In 2013, researchers at NASA Ames studied the radiation of CO(4+) in the electric arc shock tube (EAST) facility[2,8] to characterize the radiative heat flux under Venus and Mars entry conditions. They compared measurements of CO(4+) radiation with predictions made with the HARA,[9,10] HyperRad[11] and NEQAIR[12] radiation codes. When the equilibrium post-shock temperature was used, the models underestimated the measured radiation by a factor of 2. They noted that a large portion of the CO(4+) spectrum was blackbody limited. Fitting a blackbody curve to this portion of the spectrum yielded a second estimate of temperature, found to be 2 - 9 % higher than the equilibrium shock calculation. By using this second temperature, they achieved better agreement between the radiation models and the measurements, yet discrepancies remained at certain wavelengths. The purpose of this work is to evaluate and validate the radiative models for CO(4+) emission. A prior conference proceeding discussed our initial efforts.[13] Since the publication of this proceeding, several important adjustments have been made to the experimental approach. First, spectrally resolved emission measurements are now available down to approximately 140 nm. Second, the plasma torch operating conditions have been altered to ensure that the plasma is axisymmetric and remains unperturbed by the presence of the VUV emission system.

*Assistant Professor, Laboratoire EM2C, CNRS, CentraleSupélec, AIAA Member
†AIAA Member
‡Graduate Student, CentraleSupélec, AIAA Member
§Professor, Laboratoire EM2C, CNRS, CentraleSupélec, AIAA Associate Fellow
¶Sr. Research Scientist, Aerothermodynamics Branch, NASA Ames Research Center, AIAA Associate Fellow

II. Radiation transition probabilities of CO(4+)

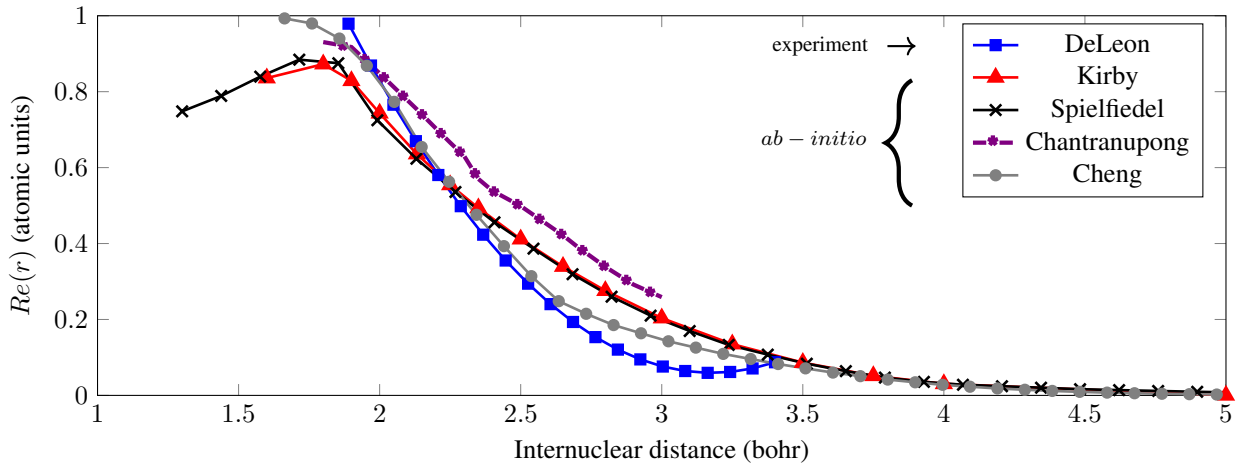

Figure 1: Electronic transition moment function ($Re(r)$) taken from Kirby and Cooper,[14] Spielfiedel et al,[15] Chantranupong et al,[16] Cheng et al[17] and DeLeon.[18,19]

For the analysis presented here, all experimental results are compared with simulations obtained using SPECAIR.[20–22] The spectral positions of the CO(4+) lines are calculated with the Dunham expansion coefficients of Farrenq et al[23] and Simmons et al.[24] Transitions between levels $\nu' = 0, 23$ of the excited state and $\nu'' = 0, 41$ of the ground state are included in the calculation. The Einstein coefficients for each rovibrational transition are calculated using the method outlined in Laux and Kruger.[25]

For these calculations, the Rydberg-Klein-Rees (RKR) method was first used to determine the potential energy curves for the X and A states of CO. The vibrational wavefunctions were then calculated. Finally, the electronic transition moment $Re(r)$ was taken from Kirby and Cooper[14] and Spielfiedel et al.[15] Both of these ETMF's are the result of *ab-initio* calculations. Figure 1 shows a comparison of these two electronic transition moments, as well as several others available in the literature. To comply with the convention outlined by Whiting,[26] the data of Kirby and Cooper have been divided by a factor of $\sqrt{2}$. For this paper, we will only analyze the ETMF's of Kirby and Cooper and Spielfiedel which are quite close - to within 5%. In the sections that follow, we will therefore use the ETMF of Spielfiedel for the calculations and treat these two ETMFs as identical. The remaining ETMF's present in Fig. 1 will be tested against the experimental data in a forthcoming publication.

III. Experiment

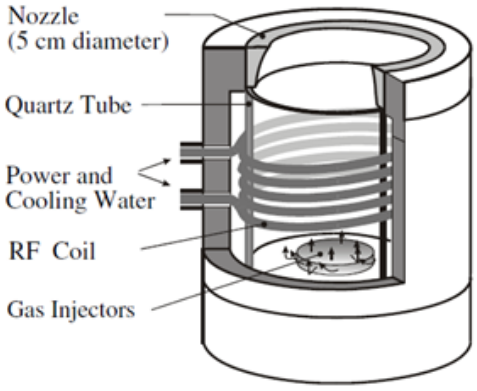

Figure 2: Plasma torch head and nozzle assembly. The gas injectors include radial, swirl and axial injectors.

The plasma torch facility is a TAFA Model 66 inductively coupled plasma (ICP) torch powered by a 120 kVA radio frequency LEPEL Model T-50-3 power supply. The power supply operates at 4 MHz and provides a maximum of 12 kV DC and 7.5 A to the oscillator plates. Details of the plasma torch facility are provided in previous publications.[20,27] For the experiments presented here, a 5-cm diameter exit nozzle was used. The plasma at the exit of the torch is at atmospheric pressure. Figure 2 shows a schematic of the facility. Radial, swirl and axial gas injectors can be used for gas injection. Calibrated flow meters from Bronkhorst (F-202AV, F-201AC, F-201CV) are used to control the mass flow rate of each gas through the system. A flow rate of 3.79 g/s of Ar was pre-mixed with 0.352 g/s of CO_2 and injected into the torch. As a percentage of the total flow rate, 54% was injected via radial injectors and 37% was injected via swirl injectors. A small amount of axial injection ($\sim$ 10%) of pure argon was also used. This small amount of axial injection was found to enhance plasma stability during operation. The reported value of 3.79 g/s argon injected includes this axial component.

Temperature measurements were obtained from the absolute intensity of emission lines of atomic carbon (833 nm), oxygen (777 nm) and argon (764 nm). These measurements were made using a UV-VIS spectrometer (Acton SpectraPro 500i), intensified PI-MAX camera and imaging setup. A longpass filter was installed in the optical path to suppress higher order diffraction interferences. The imaging system is comprised of two parabolic mirrors and a periscope to image the spectrometer slit across the jet profile. Intensity measurements are Abel-inverted to provide spatially resolved intensity measurements. The procedure for these emission-based temperature measurements is documented in Ref. 20. The analysis relies upon the assumption of thermochemical equilibrium and rotational symmetry of the plasma jet. It also assumes that the atomic emission used for the temperature analysis is optically thin.

A. VUV spectrometer

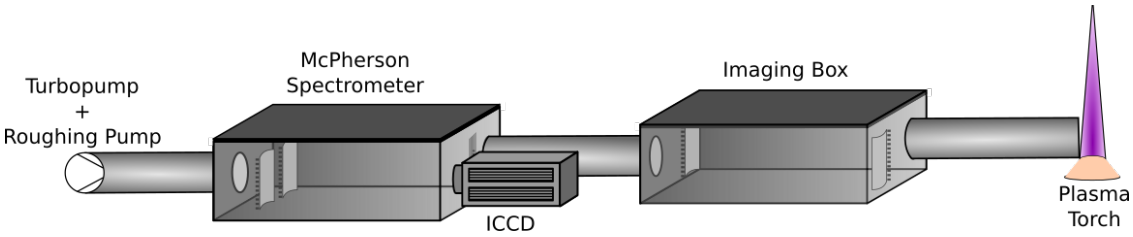

(a) VUV spectrometer and imaging system used for measurements of CO(4+).

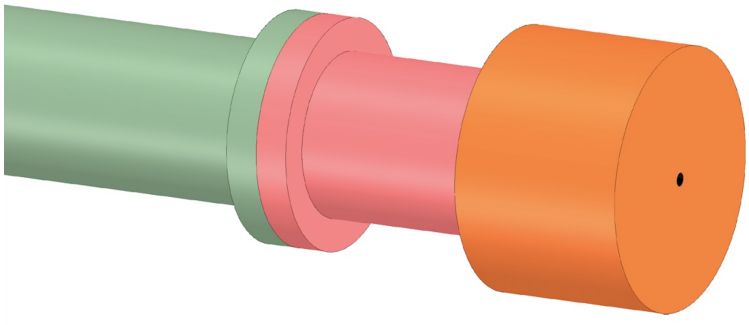

(b) Diagram showing the final tube protruding from the imaging box and coming into contact with the plasma.

Figure 3

The spectrometer and imaging system used for VUV measurements are shown in Figure 3a. The spectrometer is a McPherson VUV spectrometer (Model 218). An imaging box made of steel is attached to the spectrometer. Two spherical mirrors of 50 cm focal length inserted into this box are used to image the slit onto the torch - the spectrometer slit and torch are located at the focus of each mirror and there is therefore no image magnification. These mirrors are coated with the Acton Optics #1200 coating for 120 nm. The VUV system provides line-of-sight measurements along

the chord intersecting the plasma centerline, 2.5 cm downstream of the nozzle exit. For comparing measurements with SPECAIR calculations, the radiative transport equation is solved along the line-of-sight using the temperature profile measured using a UV-VIS spectrometer.

An overview of the VUV emission system is shown in Fig. 3a. Through the use of a rotary vane roughing pump and a turbopump (80 liters/sec), the system was pumped down to a pressure of approximately 5.0×10^{-5} Torr for all tests. The rotary vane pump was equipped with a zeolite adsorbent filter to prevent oil backstreaming into the optical system. An argon purge was used to remove oxygen from the final 10 cm of the optical path that is not under vacuum. A MgF_2 window separated this argon purged section from the primary section under vacuum. A diagram of this final 10 cm section is shown in Fig. 3b. The portion in green is under vacuum and was manufactured out of PEEK, a vacuum compatible material. The portions in red and orange are under an argon purge. The portion highlighted in orange is water-cooled copper, whereas the portion highlighed in red is manufactured out of Teflon. The materials PEEK and Teflon were chosen in order to provide electrical isolation from the torch head which rests at 10 kV. A continuous argon purge was run at a pressure slightly above 1 atm to prevent oxygen from leaking into the system. Pressure relief ports were drilled in the red teflon piece to permit a portion of the argon flush to exit via these holes, rather than entirely into the plasma. The remaining portion exited through the final viewing hole, directly entering the plasma jet. The final viewing hole in the water-cooled copper piece is 2 mm in diameter. The optical system was focused in the center of the plasma jet, 2.5 cm from the copper surface.

For calibration in absolute intensity an Optronics OL550 Tungsten ribbon lamp was used for wavelengths above 400 nm. An argon mini-arc discharge, with calibration traceable to NIST standards between 120 and 400 nm,[28] was used for wavelengths below 400 nm. In order to calibrate the system using the argon discharge, a modification of the VUV system was required. The final 10 cm of the imaging line was replaced with an adaptor to mount the system directly to the discharge housing. The sliding tube protruding from the imaging box and holding this entire assembly was adjusted so that the argon discharge emission was located at the system focus. A diaphragm placed in the imaging box served as the limiting aperture of the system so that the collection solid angle was the same for both the measurements made in the plasma torch and the calibration measurements.

IV. Results

A. Temperature measurements

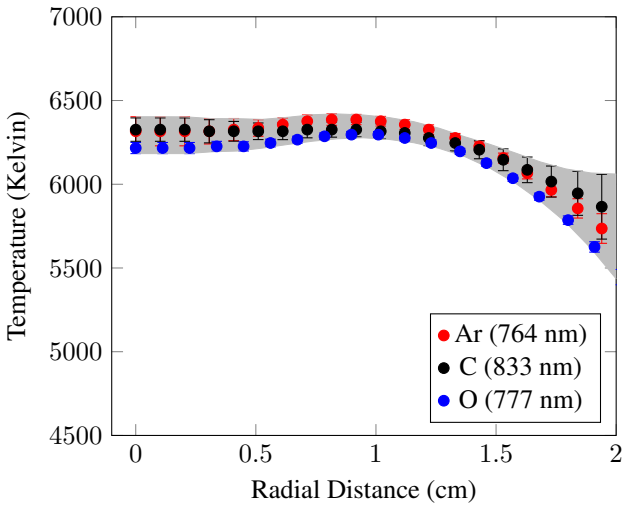

Figure 4: Temperatures obtained by measuring absolute emission from several atomic features. Uncertainty bars are included in the figure. The grey region is bounded by the maximum and minimum temperature profiles based upon the atomic measurements.

Figure 4 shows the temperature measurements for the mixture studied here. The difference in the nominal temperatures between the argon, carbon and oxygen lines is approximately 85 K. We therefore treat the plasma to be in equilibrium and apply the maximum uncertainty range, highlighted in Fig. 4. This range will be used later in the SPECAIR calculations to determine maximum and minimum emission spectra. Figure 5 shows the chemical com-

position of the plasma determined with NASA CEA[29] and using the nominal temperature from the argon 764 nm line.

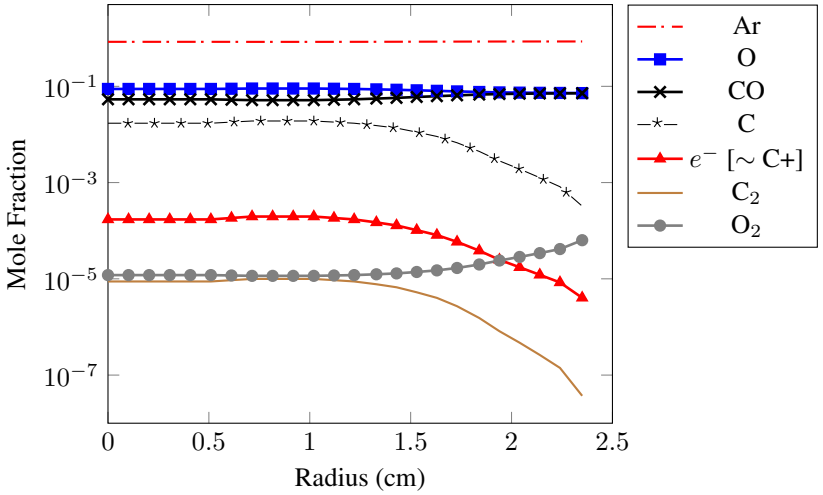

Figure 5: Equilibrium mole fractions as a function of radial distance. The calculations were done using NASA CEA[29] based upon the temperature profile measured using the argon 764 nm line. The electron mole fraction is approximately equal to the C^+ mole fraction.

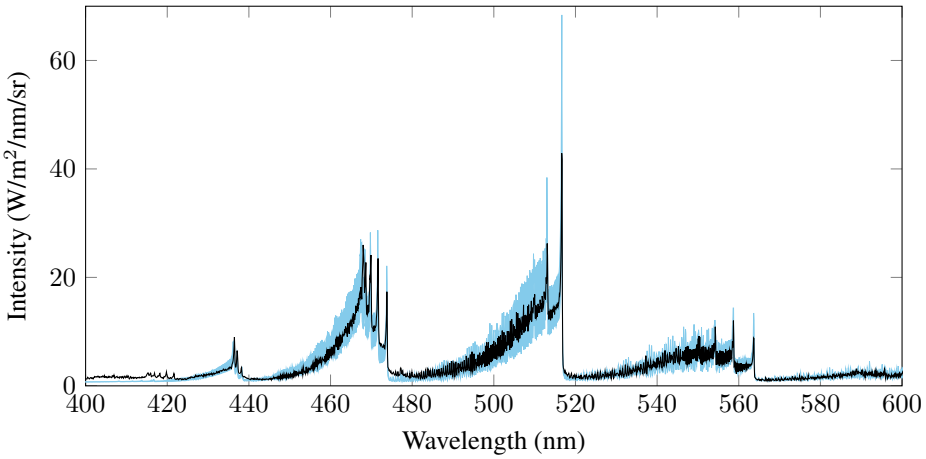

Figure 6: Comparison between measured C_2 Swan emission (black) and the SPECAIR calculation (blue). The SPECAIR calculation is bounded by the maximum and minimum intensities possible given the uncertainties in the temperature measurements. A small offset of 0.7 $W/m^2/nm/sr$ was added to the SPECAIR spectrum.

As additional confirmation that the plasma is in thermochemical equilibrium, we measured C_2 $d\,^3\Pi_g - a\,^3\Pi_u$ (Swan system) emission using the UV/VIS spectrometer setup. A grating of 600 grooves/mm blazed at 300 nm was used and the slit function had a FWHM of approximately 0.2 nm. A long pass filter ($\lambda > 350nm$) was also used to suppress higher order interferences within the spectrometer. These measurements were compared with SPECAIR predictions based upon the measured temperature profiles of Fig. 4. SPECAIR modeling of C_2 Swan radiation has been previously validated by Caillault et al.[30] A small offset of 0.7 $W/m^2/nm/sr$ was added to the SPECAIR spectrum to compensate for a small continuum that is not modeled. The mole fraction of C_2 is on the order of $5-10\times10^{-6}$ (Figure 5). Figure 6 shows a comparison between the measured and computed spectra. The good agreement is consistent with the plasma being in thermochemical equilibrium.

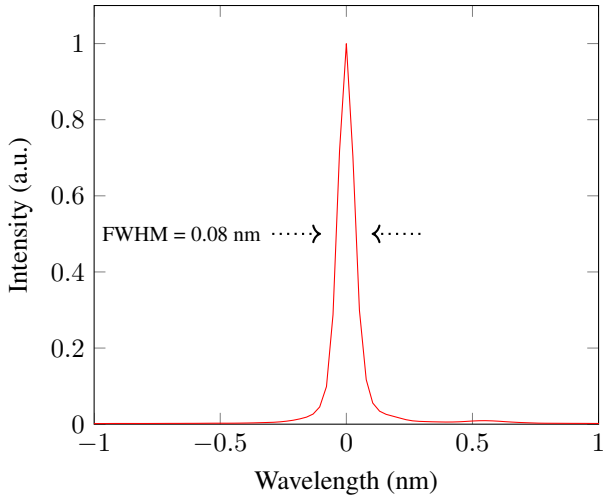

Figure 7: Measured slit function of the VUV system.

B. VUV measurements

To verify that the VUV system did not perturb the central portion of the plasma responsible for the measured emission, measurements were made in the UV/VIS region of the spectrum but using the VUV spectrometer. The measurements were found to be in agreement with Fig. 6, thus indicating that the presence of the water-cooled copper piece adjacent to the plasma does not perturb the central region responsible for the emission.

For the VUV measurements, a high-resolution 2400 grooves/mm grating was used in the VUV spectrometer. The slit function has an approximate FWHM of 0.08 nm and is shown in Figure 7 for reference. Figure 8 shows the comparison between the measured spectrum and SPECAIR calculations based upon the ETMF from Spielfiedel.[15] Note that the C_2 $D^1\Sigma_u^+ - X^1\Sigma_g^+$ (Mulliken system) is included in SPECAIR calculations and appears at 230 nm. We used the model of Bruna and Wright for this molecular system.[31] Figure 9 shows the predicted C_2 Mulliken emission given the measured temperature profile. For these plots, the uncertainty in the temperature measurements is carried through the SPECAIR calculation. The bounds on the SPECAIR calculation correspond to the minimum and maximum possible temperature based upon the measured temperature profile shown in Fig. 4. The Spielfiedel ETMF agrees within the error bars from between 162 - 210 nm. Concerning the Spielfiedel ETMF calculations, the discrepancy with the experimental measurements below 162 nm can be accounted for by cold gas absorption in the boundary layer. Sources of radiation that could cause the discrepancy above 210 nm were checked, including O_2 Schumann-Runge from entrained oxygen and carbon bound-free, though neither were strong enough to account for the difference. Thus, he discrepancy above 210 nm may indicate that Spielfiedel's ETMF should be reevaluated for this region of the spectrum.

V. Conclusion

This paper presents VUV experimental data of CO(4+) emission and assesses the performance of radiation transition probabilities obtained from the ETMF of Kirby and Cooper. A McPherson VUV spectrometer was used to spectrally analyze the emission coming from an atmospheric pressure plasma torch facility. To avoid oxygen absorption from the surrounding air, a specially designed system was put in place to make measurements down to 140 nm. The temperature of the plasma was measured using atomic emission lines. These temperature measurements were used to predict the C_2 Swan emission and found to be consistent with measured emission spectra, suggesting the plasma to be in chemical and thermal equilibrium.

At lower wavelengths (< 165 nm), absorption from cold gas (likely some combination of CO_2 and O_2) causes the signal to drop off. At these lower wavelengths, the spectra are also heavily optically thick. We find that the ETMFs of Kirby and Cooper or Spielfiedel predict very well the emission coming from the CO(4+) bands between 162-210 nm. A forthcoming paper will discuss these results in more detail, including a comparison between the experimental measurements and SPECAIR calculations made using additional ETMF's found in the literature.

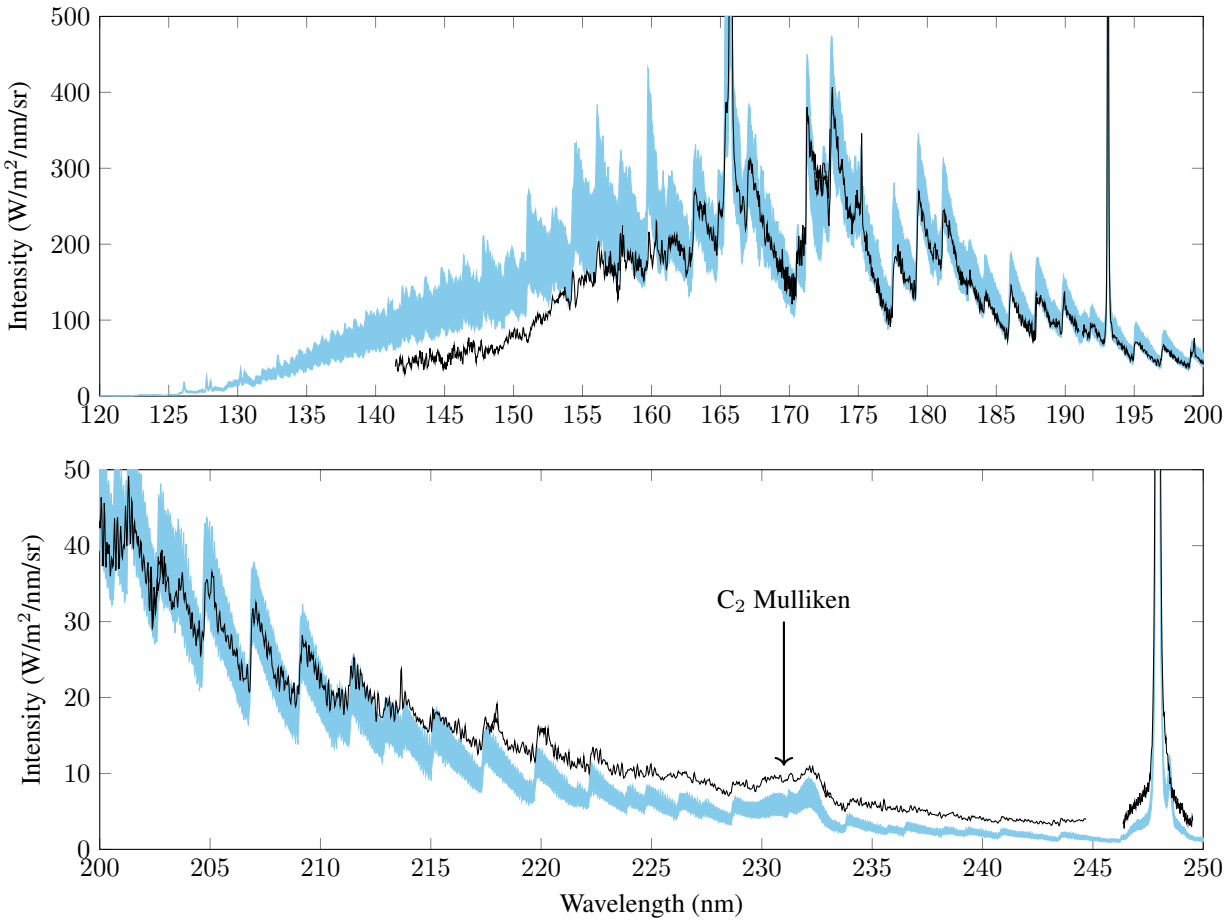

Figure 8: Experiment (black) and SPECAIR calculations (blue) based upon the Spielfiedel electronic transition moment function.

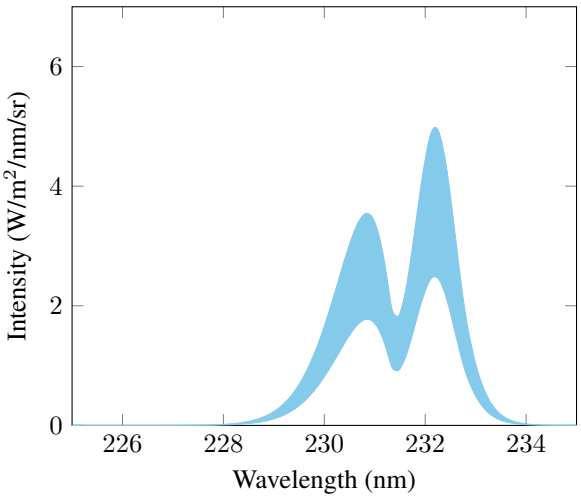

Figure 9: Predicted C_2 Mulliken emission given measured temperature profile

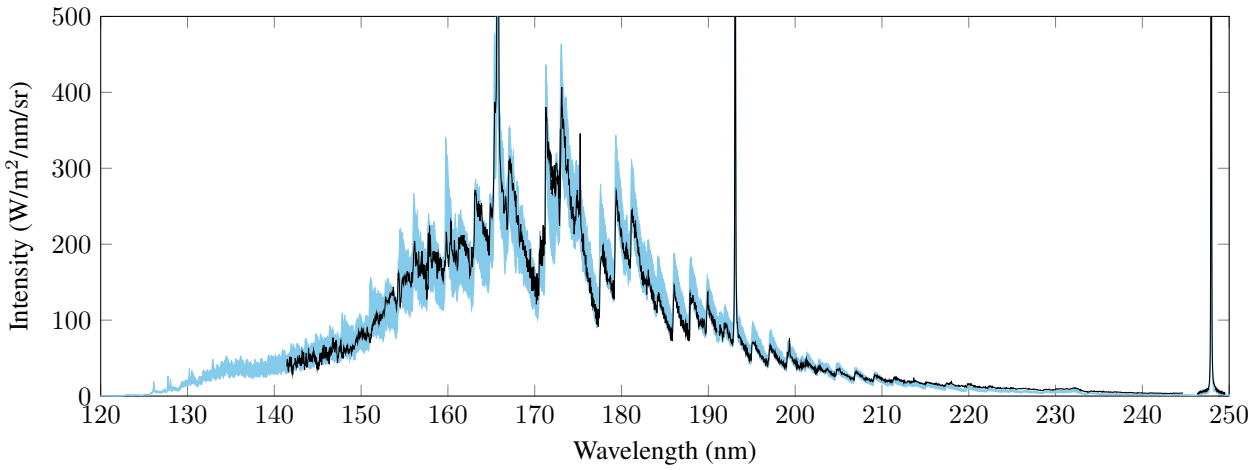

Figure 10: Same as Fig. 8 but adding 0.1 mm of cold air absorption via the O_2 Schumann-Runge system.

Acknowledgments

We would like to acknowledge the contributions of Carolyn Jacobs, Umar A Sheikh, Richard Morgan and Victor Gondret who participated in the development of this VUV system. The VUV spectrometer was obtained as part of an International NASA Space Act Agreement for Equilibrium radiation measurements. Augustin Tibère-Inglesse was supported by a CIFRE doctoral grant (number 42701092/20160218/JSE) with ArianeGroup (technical monitor: Laurent Visconti).

References

[1]W.C. Pitts and R.M. Wakefield. Performance of entry heat shields on Pioneer Venus probes. *Journal of Geophysical Research*, 85(A13):8333–8337, 1980.

[2]B.A. Cruden, D. Prabhu, and R. Martinez. Absolute radiation measurement in Venus and Mars entry conditions. *Journal of Spacecraft and Rockets*, 49(6):1069–1079, 2012.

[3]D. Bose, J.H. Grinstead, D.W. Bogdanoff, and M.J. Wright. Shock Layer Radiation Measurements and Analysis for Mars Entry. Technical Report AIAA 2019-3006, NASA Ames Research Center, 2009.

[4]J.H. Grinstead, M.J. Wright, D.W. Bogdanoff, and G.A. Allen. Shock radiation measurements for Mars aerocapture radiative heating analysis. *Journal of Thermophysics and Heat Transfer*, 23(2):249–255, 2009.

[5]M.K. Lockwood et al. Systems analysis for a Venus aerocapture mission. Technical Report TM-2006-214291, NASA, 2006.

[6]M.K. Lockwood et al. Aerocapture Systems Analysis for a Titan Mission. Technical Report TM-2006-214273, NASA, 2006.

[7]J.L. Hall, M.A. Noca, and R.W. Bailey. Cost-benefit analysis of the aerocapture mission set. *Journal of Spacecraft and Rockets*, 42(2):309–320, 2005.

[8]A.M. Brandis, C.O. Johnston, B.A. Cruden, D.K. Prabhu, A.A. Wray, Y. Liu, D.W. Schwenke, and D. Bose. Validation of CO 4th positive radiation for Mars entry. *Journal of Quantitative Spectroscopy and Radiative Transfer*, 121:91 – 104, 2013.

[9]C.O. Johnston, B.R. Hollis, and K. Sutton. Non-Boltzmann modeling for air shock-layer radiation at lunar-return conditions. *Journal of Spacecraft and Rockets*, 45(5):879–890, 2008.

[10]C.O. Johnston, B.R. Hollis, and K. Sutton. Spectrum modeling for air shock-layer radiation at lunar-return conditions. *Journal of Spacecraft and Rockets*, 45(5):865–878, 2008.

[11]Y. Liu, W. Huo, A. Wray, and D. Carbon. Electron Stark broadening database for atomic N, O, and C lines. In *43rd AIAA Thermophysics Conference*, number AIAA 2012-2739, 2012.

[12]Arnold JO Whiting EE, Yen L and Paterson JA. Nonequilibrium and equilibrium radiative transport and spectra program: user manual. Technical Report NASA RP-1389, NASA Ames Research Center, Aerothermodynamics Division, 1996.

[13]Sean McGuire, Augustin Tibère-Inglesse, Christophe O. Laux, and Brett A. Cruden. Carbon monoxide radiation in an equilibrium plasma torch facility. In *AIAA Scitech 2019 Forum*, 2019.

[14]Kate Kirby and David L. Cooper. Theoretical study of low-lying $^1\Sigma^+$ and $^1\Pi$ states of CO. II. Transition dipole moments, oscillator strengths, and radiative lifetimes. *The Journal of Chemical Physics*, 90(9):4895–4902, 1989.

[15]A. Spielfiedel, W. Tchang-Brillet, F. Dayou, and N. Feautrier. *Ab-initio* calculation of the dipole transition moment and band oscillator strengths of the CO (A-X) transition. *Astronomy and Astrophysics*, 346:699–704, 1999.

[16]Lek Chantranupong, K. Bhanuprakash, Michael Honigmann, Gerhard Hirsch, and Robert J. Buenker. A configuration interaction study of the oscillator strengths for various low-lying transitions of the co molecule. *Chemical Physics*, 161(3):351 – 362, 1992.

[17]Junxia Cheng, Hong Zhang, and Xinlu Cheng. Spectral Study of $A^1\Pi$ - $X^1\Sigma^+$ Transitions of CO Relevant to Interstellar Clouds. *The Astrophysical Journal*, 859(1):19, may 2018.

[18]R. L. DeLeon. CO (A–X) electric dipole transition moment. *The Journal of Chemical Physics*, 89(1):20–24, 1988.

[19]R. L. DeLeon. Erratum: CO (A–X) electric dipole transition moment [j. chem. phys. 89, 20 (1988)]. *The Journal of Chemical Physics*, 91(9):5859–5860, 1989.

[20]C.O. Laux. *Optical Diagnostics and Radiative Emission of Air Plasmas*. PhD thesis, Stanford University, Dept. of Mechanical Engineering, 1993.

[21]C O Laux, T G Spence, C H Kruger, and R N Zare. Optical diagnostics of atmospheric pressure air plasmas. *Plasma Sources Science and Technology*, 12(2):125, 2003.

[22]SPECAIR, Software Package, Ver. 3.0, SpectralFit S.A.S., `http://www.spectralfit.com`.

[23]R. Farrenq, G. Guelachvili, A.J. Sauval, N. Grevesse, and C.B. Farmer. Improved Dunham coefficients for CO from infrared solar lines of high rotational excitation. *Journal of Molecular Spectroscopy*, 149(2):375 – 390, 1991.

[24]J.D. Simmons, A.M. Bass, and S.G. Tilford. The fourth positive system of carbon monoxide observed in absorption at high resolution in the vacuum ultraviolet region. *Astrophysical Journal*, 155:345–358, 1969.

[25]C.O. Laux and C.H. Kruger. Arrays of radiative transition probabilities for the N_2 first and second positive, NO beta and gamma, N_2^+ first negative, and O_2 Schumann-Runge band systems. *Journal of Quantitative Spectroscopy and Radiative Transfer*, 48(1):9 – 24, 1992.

[26]E.E. Whiting, A. Schadee, J.B. Tatum, J.T. Hougen, and R.W. Nicholls. Recommended conventions for defining transition moments and intensity factors in diatomic molecular spectra. *Journal of Molecular Spectroscopy*, 80(2):249 – 256, 1980.

[27]M.E. MacDonald, C.M. Jacobs, C.O. Laux, F. Zander, and R.G. Morgan. Measurements of air plasma/ablator interactions in an inductively coupled plasma torch. *Journal of Thermophysics and Heat Transfer*, 29(1):12–23, 2014.

[28]J.Z. Klose, J.M. Bridges, and W.R. Ott. Radiometric calibrations of portable sources in the vacuum ultraviolet. *Journal of Research of the National Bureau of Standards*, 93(1):21–39, 1988.

[29]B. J. McBride and S. Gordon. Computer program for calculating and fitting thermodynamic functions. Technical report, NASA RP-1271, 1992.

[30]L. Caillault, J. Andreasson, J. Risberg, and C. Laux. Modeling the spectral radiation of a methane/nitrogen plasma test case 4. *European Space Agency, (Special Publication) ESA SP*, 629, 11 2006.

[31]Pablo J. Bruna and James S. Wright. Theoretical study of the transition probabilities of the doubly-excited states $E^1\Sigma_g^+$ of C_2 and $2^2\Sigma_g^+$ of C_2^+. *The Journal of Physical Chemistry*, 96(4):1630–1640, 02 1992.